Entanglement swapping using telecom-band photons generated in fibers

Hiroki Takesue[1,2] **and Benjamin Miquel**[1,3]

[1]*NTT Basic Research Laboratories, NTT Corporation, 3-1 Morinosato Wakamiya, Atsugi, 243-0198, Japan.*

[2]*CREST, Japan Science and Technology Agency, 4-1-8 Honcho, Kawaguchi, Saitama, 332-0012, Japan*

[3]*Ecole Normale Supèrieure,24 rue Lhomond, 75005 Paris, France.*

htakesue@will.brl.ntt.co.jp

Abstract: We report the first entanglement swapping experiment using entangled photon-pair sources based on spontaneous four-wave mixing (SFWM). The 1.5-μm band entangled photon pairs generated by SFWM in two independent 500-m dispersion shifted fibers exhibited quantum interference, thanks to the negligible walk-off between the pump and photon pairs. The use of 500-MHz gated-mode InGaAs/InP avalanche photodiodes based on the sine-wave gating technique increased the fourfold coincidence rate. As a result, the formation of an entanglement between photons from independent sources was successfully observed.

OCIS codes: (270.5565) Quantum communications; (190.4370) Nonlinear optics, fibers

References and links

1. N. Gisin and R. Thew, "Quantum communication," Nature Photon. **1**, 165-171 (2007).
2. H. Takesue, S. W. Nam, Q. Zhang, R. H. Hadfield, T. Honjo, K. Tamaki, and Y. Yamamoto, "Quantum key distribution over 40 dB channel loss using superconducting single-photon detectors," Nature Photon. **1**, 343-348 (2007).
3. H. J. Briegel, W. Dur, J. I. Cirac, and P. Zoller, "Quantum repeaters: the role of imperfect local operation in quantum communication," Phys. Rev. Lett. **81**, 5932-5935 (1998).
4. Z. S. Yuan, Y. A. Chen, B. Zhao, S. Chen, J. Schmiedmayer, and J. W. Pan, "Experimental demonstration of a BDCZ quantum repeater node," Nature **454**, 1098-1101 (2008).
5. E. Waks, A. Zeevi, and Y. Yamamoto, "Security of quantum key distribution with entangled photons against individual attacks," Phys. Rev. A **65**, 052310 (2002).
6. D. Collins, N. Gisin, and H. de Riedmatten, "Quantum relays for long distance quantum cryptography," J. Mod. Opt. **52**, 735-753 (2005).
7. J. W. Pan, D. Bouwmeester, H. Weinfurter, and A. Zeilinger, "Experimental entanglement swapping: entangling photons that never interacted," Phys. Rev. Lett. **80**, 3891-3894 (1998).
8. T. Jennewein, G. Weihs, J. W. Pan, and A. Zeilinger, "Experimental nonlocality proof of quantum teleportation and entanglement swapping," Phys. Rev. Lett. **88**, 017903 (2002).
9. H. de Riedmatten, I. Marcikic, J. A. W. van Houwelingen, W. Tittel, H. Zbinden, and N. Gisin, "Long-distance entanglement swapping with photons from separated sources," Phys. Rev. A **71**, 050302(R) (2005).
10. T. Yang, Q. Zhang, T. Y. Chen, S. Lu, J. Yin, J. W. Pan, Z. Y. Wei, J. R. Tian, and J. Zhang, "Experimental Synchronization of Independent Entangled Photon Sources," Phys. Rev. Lett. **96**, 110501 (2006).
11. H. de Riedmatten, M. Afzelius, M. U. Staudt, C. Simon, and N. Gisin, "A solid-state light-matter interface at the single-photon level," Nature **456**, 773-777 (2008).

#110358 - $15.00 USD Received 21 Apr 2009; revised 7 Jun 2009; accepted 9 Jun 2009; published 11 Jun 2009

12. P. G. Kwiat, K. Mattle, H. Weinfurter, A. Zeilinger, A. V. Sergienko, and Y. Shih, "New high-intensity source of polarization-entangled photon pairs." Phys. Rev. Lett. **75**, 4337-4341 (1995).
13. P. G. Kwiat, E. Waks, A. G. White, I. Appelbaum, and P. H. Eberhard, "Ultrabright source of polarization-entangled photons," Phys. Rev. A **60**, R773-R776 (1999).
14. G. Ribordy, J-D. Gautier, H. Zbinden, and N. Gisin, "Performance of InGaAs/InP avalanche photodiodes as gated-mode photon counters," Appl. Opt. **37**, 2272-2277 (1998).
15. S. Tanzilli, W. Tittel, H. de Riedmatten, H. Zbinden, P. Baldi, M. DeMicheli, D. B. Ostrowsky, and N. Gisin, "PPLN waveguide for quantum communication, " Eur. Phys. J. D 18, 155-160 (2002).
16. A. Yoshizawa, R. Kaji, and H. Tsuchida, "Generation of polarization-entangled photon pairs at 1550 nm using two PPLN waveguides," Electron. Lett. **39**, 621-622 (2003).
17. H. Takesue, K. Inoue, O. Tadanaga, Y. Nishida, and M. Asobe, "Generation of pulsed polarization-entangled photon pairs in a 1.55-μm band with a periodically poled lithium niobate waveguide and an orthogonal polarization delay circuit," Opt. Lett. **30**, 293-295 (2005).
18. M. Halder, A. Beveratos, N. Gisin, V. Scarani, C. Simon, and H. Zbinden, "Entangling independent photons by time measurement," Nature Phys. **3**, 692-695 (2007).
19. M. Fiorentino, P. L. Voss, J. E. Sharping, and P. Kumar, "All-fiber photon-pair source for quantum communications," IEEE Photon. Technol. Lett. **14**, 983-985 (2002).
20. H. Takesue and K. Inoue, "Generation of polarization entangled photon pairs and violation of Bell's inequality using spontaneous four-wave mixing in fiber loop," Phys. Rev. A **70**, 031802(R) (2004).
21. X. Li, P. L. Voss, J. E. Sharping, and P. Kumar, "Optical fiber-source of polarization-entangled photons in the 1550 nm telecom band," Phys. Rev. Lett. **94**, 053601 (2005).
22. H. Takesue and K. Inoue, "Generation of 1.5-μm band time-bin entanglement using spontaneous fiber four-wave mixing and planar lightwave circuit interferometers," Phys. Rev. A **72**, 041804(R) (2005).
23. H. Takesue and K. Inoue, "1.5-μm band quantum-correlated photon pair generation in dispersion-shifted fiber: suppression of noise photons by cooling fiber," Opt. Express **13**, 7832-7839 (2005).
24. J. Fulconis, Q. Alibart, W. J. Wadsworth, and J. G. Rarity, "Quantum interference with photon pairs using two micro-structured fibres," New J. Phys. **9**, 276 (2007).
25. H. Takesue, "1.5-μm band Hong-Ou-Mandel experiment using photon pairs generated in two independent dispersion shifted fibers," Appl. Phys. Lett. **90**, 204101 (2007).
26. N. Namekata, S. Sasamori, and S. Inoue, "800 MHz single-photon detection at 1550-nm using an InGaAs/InP avalanche photodiode operated with a sine wave gating," Opt. Express **14**, 10043-10049 (2006).
27. J. Brendel, N. Gisin, W. Tittel, and H. Zbinden, "Pulsed energy-time entangled twin-photon source for quantum communication," Phys. Rev. Lett. **82**, 2594-2597 (1999).
28. H. de Riedmatten, I. Marcikic, V. Scarani, W. Tittel, H. Zbinden, and N. Gisin, "Tailoring photonic entanglement in high-dimensional Hilbert spaces," Phys. Rev. A **69**, 050304(R) (2004).
29. M. Suzuki, H. Tanaka, N. Edagawa, K. Utaka, and Y. Matsushima, "Transform-limited optical pulse generation up to 20-GHz repetition rate by a sinusoidally driven InGaAsP electroabsorption modulator," J. Lightwave Technol. **11**, 468-473 (1993).
30. P. R. Tapster and J. G. Rarity, "Photon statistics of pulsed parametric light," J. Mod. Opt. **45**, 595-604 (1998).
31. H. de Riedmatten, V. Scarani, I. Marcikic, A. Acin, W. Tittel, H. Zbinden, and N. Gisin, "Two independent photon pairs versus four-photon entangled states in parametric down conversion," J. Mod. Opt. **51**, 1637-1649 (2004).
32. R. Hanbury Brown and R. Q. Twiss, "Correlation between photons in two coherent beams of light," Nature **177**, 27-29 (1956).
33. C. K. Hong, Z. Y. Ou, and L. Mandel, "Measurement of subpicosecond time intervals between two photons by interference" Phys. Rev. Lett. **59**, 2044-2046 (1987).
34. A. Politi, M. J. Cryan, J. G. Rarity, S. Yu, and J. L. O'Brien, "Silica-on-silicon waveguide quantum circuits," Science **320**, 646-649 (2008).
35. M. Halder, private communication.
36. N. Namekata, S. Adachi, and S. Inoue, "1.5 GHz single-photon detection at telecommunication wavelengths using sinusoidally gated InGaAs/InP avalanche photodiode," Opt. Express **17**, 6275-6282 (2009).
37. S. D. Dyer, M. J. Stevens, B. Baek, and S. W. Nam,"High-efficiency, ultra low-noise all-fiber photon-pair source," Opt. Express 16, 9966-9977 (2008).
38. H. Takesue, Y. Tokura, H. Fukuda, T. Tsuchizawa, T. Watanabe, K. Yamada, and S. Itabashi, "Entanglement generation using silicon wire waveguide," Appl. Phys. Lett. **91**, 201108 (2007).

1. Introduction

Remarkable progress has been made on quantum key distribution (QKD) systems over optical fiber in recent years [1]. The key distribution distance of a point-to-point QKD has now reached 200 km [2]. It is believed that the most effective way of extending the key distribution distance

#110358 - $15.00 USD Received 21 Apr 2009; revised 7 Jun 2009; accepted 9 Jun 2009; published 11 Jun 2009

further is to employ quantum repeaters [3, 4]. However, it is still difficult to construct practical quantum repeater systems with the currently available technologies. A simpler method for extending the key distribution distance to ∼400 km of fiber is to use a quantum relay [5, 6], which is a QKD using entanglement distributed via entanglement swapping [7, 8, 9, 10]. To realize this, entanglement swapping in the 1.5-μm telecom band is an important first step. In addition, if we implement entanglement swapping with other sophisticated technologies such as a quantum memory [11], we can realize fully scalable quantum communication based on quantum repeaters.

Most previous experimental entanglement swapping [7, 8, 10] used short-wavelength photon pairs generated by spontaneous parametric downconversion (SPDC) in nonlinear crystals [12, 13], while the Bell state measurement was undertaken in the 1.3-μm band in [9]. However, entanglement swapping in the 1.5-μm band has proved challenging because of the immature status of the components needed for multi-coincidence experiments at this wavelength. One such component is a single photon detector. To date, InGaAs/InP avalanche photodiodes (APD) operated in a gated mode have been most commonly used as single photon detectors in the 1.5-μm band [14]. However, the gate frequency of an InGaAs/InP-based photon detector is typically smaller than 10 MHz, which means that the effective clock frequency of the whole setup is limited by this relatively slow gate frequency and thus it is difficult to increase the fourfold coincidence rate.

Another component needed for entanglement swapping is a 1.5-μm entanglement source that generates indistinguishable photon pairs. Currently, the most widely used entanglement source for the 1.5-μm band is based on SPDC in a periodically poled lithium niobate (PPLN) waveguide [15, 16, 17, 18]. In the SPDC process in the PPLN waveguide, a large walk-off between a short wavelength pump pulse and a 1.5-μm photon pair causes the photon pair to exhibit timing jitter. As a result, it is generally difficult to obtain quantum interference using photons from independent sources based on PPLN waveguides.

Recently, a group from Geneva University reported the first entanglement swapping experiment to use 1.5-μm band energy-time entangled photon pairs [18]. They used SPDC in PPLN waveguides, together with very narrow filters and a low-jitter superconducting single photon detector, with which they managed to suppress the walk-off problem and successfully obtained indistinguishable photon pairs from independent sources.

Here, we report a 1.5-μm band entanglement swapping experiment based on a different scheme. Our scheme uses time-bin entangled photons, which are pulsed entangled states suitable for high-clock-rate systems, generated by spontaneous four-wave mixing (SFWM) in dispersion shifted fibers (DSF) [19, 20, 21, 22, 23]. As previously demonstrated in the short wavelength band [24] and the 1.5-μm band [25], the fiber-based sources facilitated the generation of indistinguishable photon pairs. Also, the use of high-speed InGaAs APDs with a 500-MHz gate frequency, which were realized using the sine-wave gating technique [26], contributed significantly to the increase in the fourfold count rate. As a result, an entanglement was successfully formed between photons from independent fiber sources. The whole entanglement swapping setup was operated at a clock frequency as high as 500 MHz, which we believe paves the way for the realization of a quantum relay over optical fiber networks.

2. Setup

2.1. Time-bin entangled photon pair sources

Figure 1 shows the experimental setup for generating sequential time-bin entangled photon pairs [22, 27, 28]. A continuous light from an external cavity diode laser with a wavelength of 1551.1 nm was modulated into 19-ps pulses by utilizing the nonlinear attenuation characteristics of an electroabsorption (EA) modulator driven by a 10-GHz sinusoidal signal [29]. The

#110358 - $15.00 USD Received 21 Apr 2009; revised 7 Jun 2009; accepted 9 Jun 2009; published 11 Jun 2009

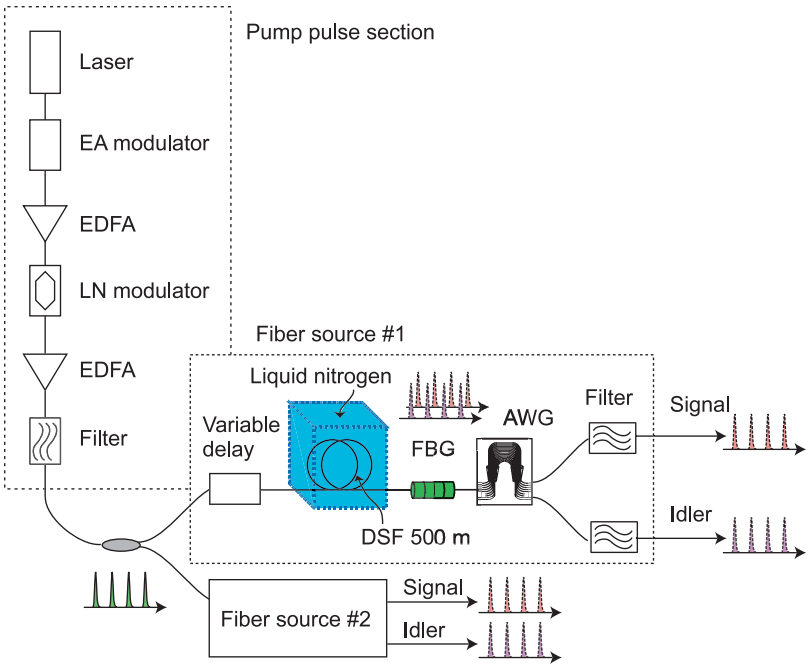

Fig. 1. Experimental setup (I) time-bin entangled photon-pair sources.

10-GHz pulse train was amplified with an erbium doped fiber amplifier (EDFA) and then the repetition frequency was reduced to 500 MHz using a lithium niobate (LN) modulator. The 500-MHz pulse train was again amplified with another EDFA, filtered to suppress amplified spontaneous emission noise, and then divided into two paths by an optical coupler. The pulse peak power in each path was approximately 0.5 W. The pulses in each path were transmitted through a variable delay line to adjust their temporal positions, and input into a 500-m DSF that was cooled by liquid nitrogen to suppress the noise photons caused by spontaneous Raman scattering. In this cooled DSF, the pulse train created sequential time-bin entangled photon pairs, whose state is approximately given by [28] $\frac{1}{\sqrt{N}}\sum_{k=1}^{N}|k\rangle_s|k\rangle_i$. Here, $|k\rangle_x$ denotes a state in which there is a photon in a temporal position k and a mode x, and N is the number of pulses in which the phase coherence of the pump pulses is preserved. The photons from each DSF were transmitted through a fiber Bragg grating (FBG) to suppress the pump, and launched into an arrayed waveguide grating (AWG) followed by optical bandpass filters to separate the signal and idler photons. The signal and idler wavelengths were 1547.9 and 1554.3 nm, respectively. The total loss of the FBG, the AWG and the bandpass filter was approximately 6 dB for each channel.

The bandwidths of the filters were both 0.2 nm, implying that the coherence time of the photon pairs was approximately 18 ps. According to [30, 31], photon pairs generated via a spontaneous parametric process become distinguishable when the pump pulse width is much larger than the coherence time of the photon pairs. With the present setup, in which the widths of the pump pulse and photon pair coherence time were almost the same, this timing jitter is well suppressed and so nearly indistinguishable photon pairs can be created. When indistinguishable photon pairs are generated, their number distribution typically becomes a thermal distribution, while distinguishable pairs have a Poissonian distribution [31]. To determine whether the photon pair was indistinguishable or not, we measured the second-order correlation function $g^{(2)}(0)$

#110358 - $15.00 USD Received 21 Apr 2009; revised 7 Jun 2009; accepted 9 Jun 2009; published 11 Jun 2009

of the idler photons using a Hanbury Brown and Twiss setup [32]. The result is shown in Fig. 2 (a). Clear photon bunching with $g^{(2)}(0) = 1.6$ was observed, indicating that photons from two independent fiber sources could exhibit quantum interference.

We also undertook two-photon interference fringe measurements for fiber sources #1 and 2. When we set the average photon pair number per pulse at 0.04, the fringe visibilities were both $\sim 70\%$.

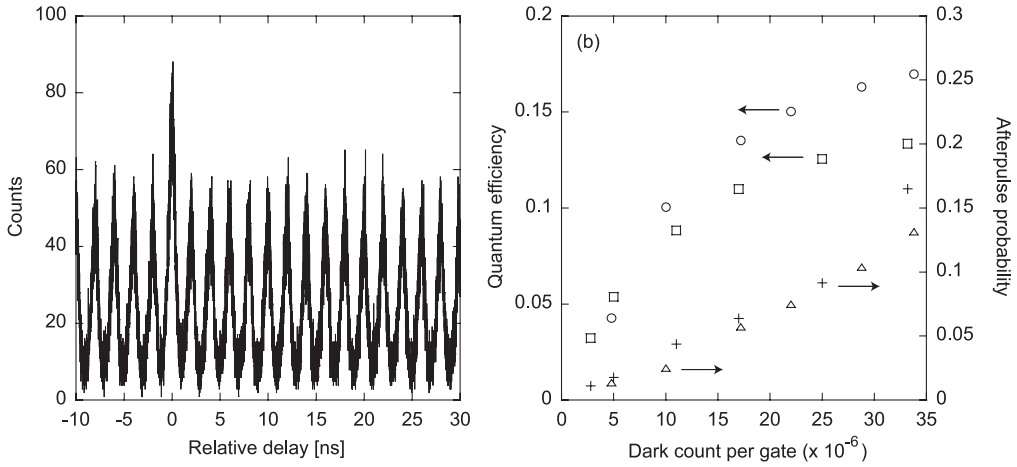

Fig. 2. (a) Result of $g_2(0)$ measurement. (b) Quantum efficiency and afterpulse probability as a function of dark count probability per gate. Squares and triangles: detector x, circles and crosses: detector y.

2.2. Coincidence measurement setup

Figure 3 shows the setup for entanglement swapping using fiber sources #1 and #2 described above. The signal photons from fiber sources #1 and #2 were sent to Alice and Bob, respectively, and the idler photons were sent to Charlie. The idler photons received by Charlie were input into a fiber beamsplitter (BS) whose output ports were connected to InGaAs/InP APDs for single photon counting. The two input and output ports of the BS are denoted as ports 1, 2, x and y, respectively, as shown in Fig. 1. The gate frequency of these APDs was as high as 500 MHz, which was made possible by using the sine-wave gating technique [26]. The quantum efficiencies and the afterpulsing probability as a function of dark count probability are shown in Fig. 2 (b). Thus, quantum efficiencies of better than 10% were obtained for both detectors with moderate dark count probabilities of $\sim 2 \times 10^{-5}$. In the following experiment, we set the quantum efficiencies and dark count probabilities per gate, respectively, at 11% and 1.8×10^{-5} for channel x, and 13% and 1.6×10^{-5} for channel y. The afterpulsing probability of the two detectors were both $\sim$4%. A polarizer was placed in front of the detector for channel x. Then, the polarization states of the idler photons were adjusted to maximize the count rate of the detector, and so the polarization states of the two idler photons were set so that they were the same.

Here we describe the Bell state measurement of a sequential time-bin entangled state using a BS and threshold detectors. The quantum state of the total system is written as

$$|S\rangle = \frac{1}{N}\left(\sum_{j=1}^{N} |j\rangle_{1s}|j\rangle_{1i}\right) \otimes \left(\sum_{k=1}^{N} |k\rangle_{2s}|k\rangle_{2i}\right), \quad (1)$$

#110358 - $15.00 USD Received 21 Apr 2009; revised 7 Jun 2009; accepted 9 Jun 2009; published 11 Jun 2009

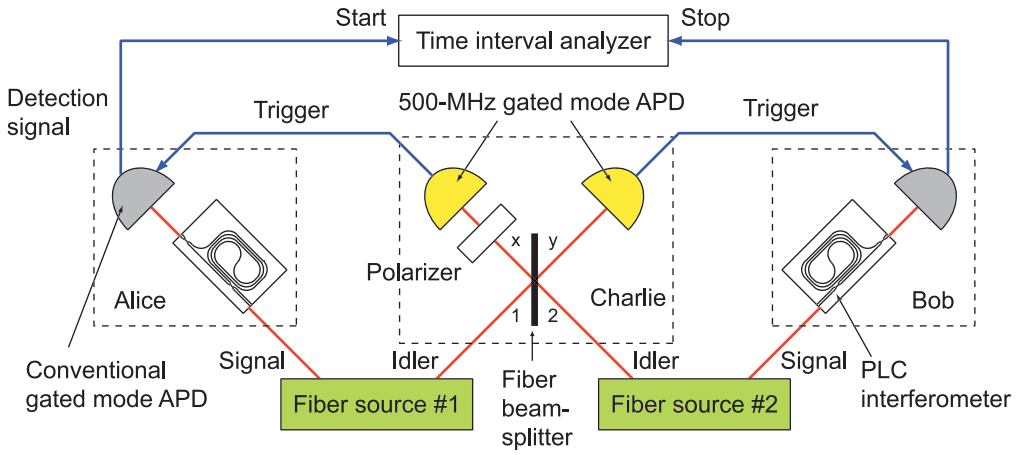

Fig. 3. Experimental setup (II) fourfold coincidence measurement.

where the first subscript denotes the fiber source number (1 or 2). This state can be rewritten using the four Bell states formed by two idler photons, $|\Phi_k^{\pm}\rangle = (|k\rangle_{1i}|k\rangle_{2i} \pm |k+1\rangle_{1i}|k+1\rangle_{2i})/\sqrt{2}$ and $|\Psi_k^{\pm}\rangle = (|k\rangle_{1i}|k+1\rangle_{2i} \pm |k+1\rangle_{1i}|k\rangle_{2i})/\sqrt{2}$, as

$$\begin{aligned} |S\rangle \quad \rightarrow \quad & \frac{1}{N\sqrt{2}} \left\{ \sum_{k=1}^{N} |k\rangle_{1s}|k\rangle_{2s}(|\Phi_k^+\rangle + |\Phi_k^-\rangle) \right. \\ & + \sum_{k=1}^{N-1} (|k\rangle_{1s}|k+1\rangle_{2s} + |k+1\rangle_{1s}|k\rangle_{2s})|\Psi_k^+\rangle \\ & \left. + (|k\rangle_{1s}|k+1\rangle_{2s} - |k+1\rangle_{1s}|k\rangle_{2s})|\Psi_k^-\rangle \right\}. \end{aligned} \tag{2}$$

Here, the states that are not observed in our coincidence measurements using 1-bit delayed interferometers are omitted for simplicity. The Bell states $|\Phi_k^{\pm}\rangle$ cannot be discriminated using a BS followed by threshold detectors, since the two input photons bunch in the same spatial and temporal mode at the BS output ports as a result of the Hong-Ou-Mandel (HOM) effect [33]. When $|\Psi_k^+\rangle$ is input into the BS, the two photons are output in the same spatial mode but in different temporal modes. This means that in theory this state can be discriminated using threshold detectors. However, the discrimination of two consecutive photon pulses in the same spatial mode requires a detector deadtime of <2 ns, which is very difficult to achieve with current single photon counting technologies. When a Bell state $|\Psi_k^-\rangle$ is input into a BS, the output state is given by $(|k\rangle_x|k+1\rangle_y - |k+1\rangle_x|k\rangle_y)/\sqrt{2}$ (the subscripts denote the output ports), implying that only this state gives a coincidence count between detectors x and y, and thus can be discriminated from the other three states. Therefore, we adjusted the temporal position of the detector gates for channels x and y to detect photons in the $(k+1)$th and the kth time slots, respectively, by which we can implement a projection measurement on a portion of $|\Psi_k^-\rangle$ (i.e. $\frac{1}{\sqrt{2}}|k+1\rangle_x|k\rangle_y$). Then, Eq. (2) shows that the two signal photons form an entangled state $(|k\rangle_{1s}|k+1\rangle_{2s} - |k+1\rangle_{1s}|k\rangle_{2s})/\sqrt{2}$.

The signal photons sent to Alice and Bob were input into 1-bit delayed interferometers fabricated with planar lightwave circuit (PLC) technology [22] followed by InGaAs/InP APDs operated in a conventional gated mode. The phase differences between the two arms of the interferometers were tuned by adjusting the temperature of the PLC substrates. The use of the PLC interferometers enabled the setup to operate stably over a long period. We confirmed that

#110358 - $15.00 USD Received 21 Apr 2009; revised 7 Jun 2009; accepted 9 Jun 2009; published 11 Jun 2009

the phases of our PLC interferometers were stable within $\pm 0.06\pi$ for at least 12 hours without any feedback control other than temperature control. In the future, we will also be able to use the PLC-based BS [34] to realize a compact BSM. Alice's and Bob's APDs were gated using detection signals from detectors x and y, respectively, owned by Charlie. Then the detection signals from Alice's and Bob's APDs were used as start and stop pulses for a time interval analyzer (TIA). As a result, the coincidence events recorded by the TIA were conditioned by the Bell state measurement at Charlie.

3. Results

We first removed the PLC interferometers and observed a HOM dip using idler photons from the two independent fiber sources. Here, the coincidence measurement at the output of the BS was conditioned by the detection of signal photons at Alice and Bob. The fourfold coincidence counts as a function of the relative delay between two idler photons is shown in Fig. 4 (a). A clear dip was observed when the relative delay was zero. The visibility of the dip was $64 \pm 8\%$. Thanks to the 500-MHz gated mode detectors, we were able to count the fourfold coincidences with an average photon pair number per pulse (~ 0.04) that was much smaller than that in our previous experiment (~ 0.14) [25]. This reduced average photon pair number resulted in fewer accidental coincidences, and thus we obtained a visibility much larger than that reported in [25] (53%). This result shows that the two photons generated in two independent DSFs that were as long as 500 m could exhibit nonclassical interference.

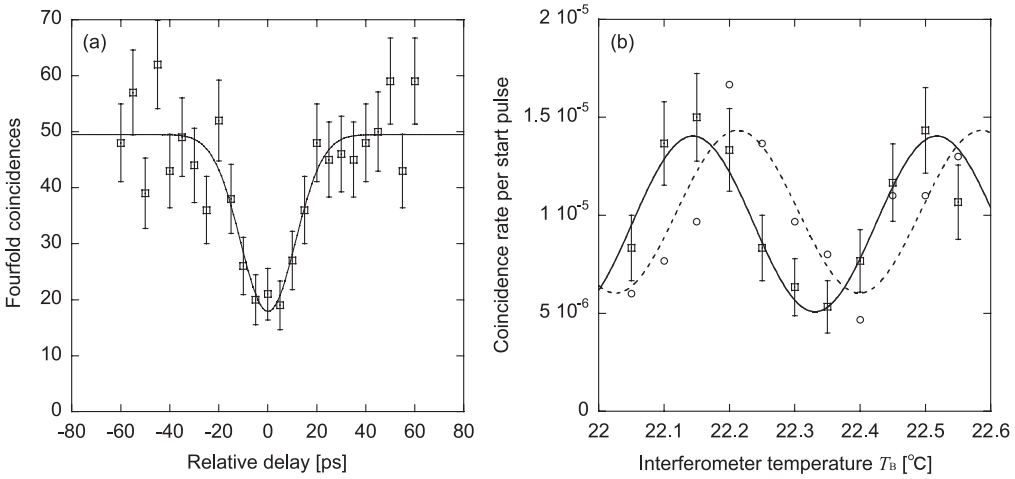

Fig. 4. (a) HOM measurement result. The vertical axis shows the fourfold coincidences obtained by the TIA for 1,000,000 start pulses. The detection signals from Alice's and Bob's detectors were used as the start and stop pulses for the TIA. Alice's and Bob's detectors were gated using the detection signal from the detectors owned by Charlie. (b) Two-photon interference fringe obtained using coincidence counts of two signal photons conditioned by Bell state measurement of idler photons. The vertical axis shows the coincidence rate per start pulse. Squares: $T_A = 32.25^\circ$C, circles: $T_A = 32.35^\circ$C. Statistical error bars are given only for the data with $T_A = 32.25^\circ$C. Note that no accidental coincidences or noise counts have been subtracted from the data shown in (a) and (b).

Next, we inserted the PLC interferometers, and observed the two-photon interference of the signal photons received by Alice and Bob. As explained above, the detection of the signal photons was triggered by the Bell state measurement undertaken at Charlie's site, which means that the coincidences observed by the TIA corresponded to fourfold coincidences observed by

#110358 - $15.00 USD Received 21 Apr 2009; revised 7 Jun 2009; accepted 9 Jun 2009; published 11 Jun 2009

the four detectors. We fixed the temperature of Alice's interferometer T_A at 32.25°C, and measured the coincidence counts while sweeping the temperature of Bob's interferometer T_B. The average photon pair number per pulse was set at the same value as that in the HOM experiment. The obtained coincidence rates are shown by squares in Fig. 4 (b). A clear modulation of coincidence was observed, which suggests that the two signal photons originating from two independent sources were now correlated. The visibility of the best-fitted curve was $47 \pm 7\%$. We would like to stress that no accidental coincidences or noise counts have been subtracted from the data shown here. To rule out the possibility that the modulation was caused by a classical correlation, we changed T_A to 32.35°C, which corresponds to an interferometer phase shift of about $\pi/2$, and undertook another two-photon interference measurement. The result is shown by the circles in Fig. 4 (b), which again showed a clear fringe with a visibility of $41 \pm 9\%$. Thus, we obtained two-photon interferences for two non-orthogonal measurement bases with visibilities better than 41%. When we subtracted the accidental coincidences, the visibilities were $124 \pm 30\%$ ($T_A = 32.25$°C) and $98 \pm 23\%$ ($T_A = 32.35$°C). Here, the accidental coincidences include the erroneous coincidences caused by the dark counts and the imperfections of the sources such as multi-photon emission and temporal distinguishability of the photon. Another factor degrading the visibility is the limited extinction ratio of the PLC interferometers, which degrades the visibility by ∼1%. Therefore, the fringe visibility after the subtraction of the accidental coincidences should be ∼99% if there are no statistical fluctuations. In reality, the large statistical fluctuation in the coincidences and accidental coincidences caused several negative points to appear in the corrected fringes, which resulted in the visibility exceeding 100%. The accidental coincidence rates were estimated by counting the coincidences caused by photons generated with different pump pulses. The measurement procedure for counting the accidental coincidences is detailed in [22]. The coincidence rate at the peak of the fringe was 0.038 Hz, which is much higher than that of the previous experiment (7.5 coincidences per hour) [18, 35]. If we assume that the two photons are in a Werner state, a visibility greater than 33% is sufficient to demonstrate entanglement [18]. Therefore, the result shown here indicates that an entanglement was formed between two signal photons originating from two independent fiber sources.

4. Discussion

We can think of two main reasons for the relatively low visibility. The probable main source of the visibility degradation is accidental coincidences caused by multi-pair emission. In our experiment, spontaneous Raman scattering (SpRS) noise, which is not suppressed even at liquid nitrogen temperature, could increase the accidental coincidence rate. With the analysis described in [23], we can estimate that the noise photons account for ∼75% of the generated photons, and this could seriously degrade the visibility. When the average correlated photon number per pulse is μ_c and the total average photon number per pulse is μ, the theoretical visibility of a HOM dip that takes account of two-pair generation is given by

$$V_{HOM2} = \frac{\mu_c + 8\mu^2}{\mu_c + 12\mu^2}. \tag{3}$$

The above equation is obtained by using a similar procedure to that described in [24]. In the present experiment with $\mu_c \simeq 0.01$ and $\mu \simeq 0.04$, this degrades the HOM visibility to ∼78%. Another possible reason is the relatively broad pump pulse, which may have led to temporal distinguishability. If the ratio between the pump pulse width and the photon pair coherence time is given by r, the expected visibility of a HOM dip obtained with SFWM-based sources is

#110358 - $15.00 USD Received 21 Apr 2009; revised 7 Jun 2009; accepted 9 Jun 2009; published 11 Jun 2009

expressed as [24]

$$V_{HOM1} = \frac{\sqrt{1+r^2}}{1+r^2/2}. \tag{4}$$

With the parameters used in this experiment, a broad pulse degrades the visibility to ∼93%. Possible other sources of visibility degradation include a large statistical fluctuation because of the low fourfold coincidence rate and a polarization drift during the measurement. We believe that a combination of the above factors resulted in the HOM visibility of 63%.

In this experiment, we directly connected the nodes without using transmission fibers. The distance of the entanglement distribution in this scheme is in reality not limited by the degradation of the signal-to-noise ratio but by the decrease in the coincidence rate. For example, if we assume that the minimum required coincidence rate is 0.01 Hz, the total length of fiber that we can insert between nodes is ∼30 km with the current setup. Thus, it remains very important to increase the coincidence rate. The most straightforward way to increase the rate is to improve the single photon detectors. For example, the use of detectors with a 1.5-GHz gate frequency [36] will be effective in improving the rate. Thus, further improvement of the 1.5-μm band single photon detectors is required if the current scheme is to be deployed for entanglement distribution over optical fiber. In addition, we expect the SpRS noise to be better suppressed if we cool the DSF to a lower temperature [37] or use SFWM in a silicon waveguide [38], so that we can realize better visibility.

We would like to emphasize the fact that we used pump pulses whose temporal width was in the ps regime, whereas most previous experiments have used fs pump pulses. The use of the relatively broad pump pulses will facilitate the synchronization of two (or more) distant pump sources, which constitutes a great advantage as regards constructing quantum communication systems in real fiber networks.

5. Conclusion

We have reported the first entanglement swapping experiment to use fiber-based entanglement sources. SFWM in 500-m DSFs pumped by a pulse train generated through the external modulation of continuous-wave laser light was used to obtain indistinguishable time-bin entangled photon pairs. The use of 500-MHz gated-mode InGaAs/InP avalanche photodiodes based on the sine-wave gating technique reduced the measurement time significantly. The formation of an entanglement between photons from independent sources was successfully observed.

Acknowledgements

The authors thank S. Inoue and N. Namekata of Nihon University for fruitful discussions on high-speed single photon detectors.

#110358 - $15.00 USD Received 21 Apr 2009; revised 7 Jun 2009; accepted 9 Jun 2009; published 11 Jun 2009